Flapping instability of a liquid jet

Antoine DELON[1], Jean-Philippe MATAS[1], Alain CARTELLIER[1]

[1]*Laboratoire des Ecoulements Géophysiques et Industriels, (CNRS/UJF/Grenoble INP), Grenoble, France*

Keywords: Flapping instability, Kelvin-Helmholtz instability, shear instability, assisted atomization

Abstract

In air assisted atomization, small droplets arise from the stripping of a liquid jet (or a film) by a fast gas stream (Lasheras & Hopfinger 2000, Eggers & Villermaux 2008). Yet, the incoming liquid jet is seemingly never fully atomized by the stripping process alone. Instead, the remaining jet experiences a flapping instability, similar to the instability observed on liquid sheet configurations: the resulting large scale structures break into large liquid lumps some distance downstream the injection. Little is known on the underlying mechanism of this instability and on the characteristics of the large drops it produces, though these large drops probably control flame extent in combustion devices. We suggest in the present study that this instability could be triggered by non-axisymmetric Kelvin-Helmholtz modes. Indeed, in coaxial injector configuration, non-axisymmetric modes of the KH instability can be observed.

First, we study the dependence of KH modes upon two control parameters, namely the liquid and gas velocities, and discuss the symmetry of these modes. Secondly, we investigate a possible link between non-symmetric modes of KH instability and the large scale instability. Finally, amplitude of the large scale oscillation is measured as a function of gas and liquid velocity.

Introduction

Assisted atomization of a liquid jet, also known as airblast atomization, is fundamental to many applications. In this process, liquid is stripped from a cylindrical jet by a fast co-current air-stream, and a spray is produced (Lasheras & Hopfinger 2000, Eggers & Villermaux 2008, Marty et al 2013). Applications range from injectors in turboreactors, to cryotechnic rocket engines with LOX/H2. This process is widely used, and has proven reliable, but the mechanism by which the liquid bulk is broken into droplets is still subject to controversy. A better understanding of the different stages of the atomization process could help improve the efficiency of combustion, and decrease the amount of emissions.

Experiments carried out on a planar mixing layer (Hong et al 2002) and on a coaxial injector (Marmottant & Villermaux 2004) have shown that the liquid break up is the result of two successive instabilities. The first instability is a shear instability, analogous to a Kelvin-Helmholtz instability but controlled by the thickness of the gas vorticity layer δ_g (Rayleigh 1879), and leads to the formation of 2D longitudinal waves at the interface between the liquid and the fast gas stream. An inviscid stability analysis, based on a realistic velocity profile including a velocity deficit at the interface, predicts the following most unstable mode wavenumber and corresponding frequency: $k=\sqrt{r}/\delta_g[\sqrt{2}+(3/2)M^{-1/2}]$ and $\omega_r=rU_g\backslash\delta_g[1+(5\sqrt{2}/2)M^{-1/2}]$ where $r=\rho_g/\rho_l$ is the gas to liquid density ratio, U_g and U_l are the respective gas and liquid velocities, and where M stands for the dynamic pressure ratio $M = \rho_g U_g^2/(\rho_l U_l^2)$. Agreement between this prediction and the measurement frequency is good (Matas et al 2011). In a coaxial geometry, the same mechanisms hold and the corresponding waves are axisymmetric: in the latter geometry though, experimental frequencies are significantly larger than predicted ones (Marmottant & Villermaux 2004), a point which is still the subject of investigation.

The waves resulting from this instability are next accelerated by the fast gas stream, and undergo a Rayleigh-Taylor transverse instability, leading to the formation of liquid ligaments. Two proposals are available for that instability, one related with the axial acceleration of waves crest (Hong et al. 2002, Varga et al. 2003) and the other one related to an acceleration normal to the interface (Marmottant & Villermaux 2004). These ligaments grow and eventually break into droplets, whose size is controlled by the thickness of ligaments, and hence the wavelength of the R-T instability.

When stripping mechanism previously described does not completely break the entire liquid jet, atomization of the liquid jet is incomplete: while small droplets are still produced in the potential cone region, far downstream the liquid jet ends up breaking into large liquid lumps. Just before its break-up, the liquid jet oscillates with a wavelength large compared to the jet diameter (figure 1). Our study is devoted to this large scale instability, called here the "flapping" instability, and more specifically about a possible link between a particular mode of the K-H instability wave and the large scale instability. Indeed, the large scale instability could be interpreted as a large scale amplification of non symmetric modes of K-H instability waves. The dependence of K-H instability modes with gas and liquid velocity is showed and confronted with the features of the flapping instability.

Nomenclature

g	gravitational constant (ms^{-2})
P	pressure (Nm^{-2})

Greek letters

Subscripts

K-H	Kelvin-Helmholtz
X_g	Gas subscript
X_l	Liquid subscript
D	Liquid nozzle diameter
Hg	Thickness of the nozzle gas ring
λ	Wavelength of large scale instability
M	Dynamic pressure ratio
C	correlation coefficient

Experimental Facility and methods

A round vertical jet is atomized by a fast coaxial annular air stream (figure 2). The profiles of air and water channels are detailed in figure 2. Air is supplied by laboratory compressed air through a mass flow-meter (Brooks Instruments) and solenoid valve, and water is supplied by an overflowing tank placed at a few meters height in order to provide constant head and passes through an oval wheel flow meter (OVAL).

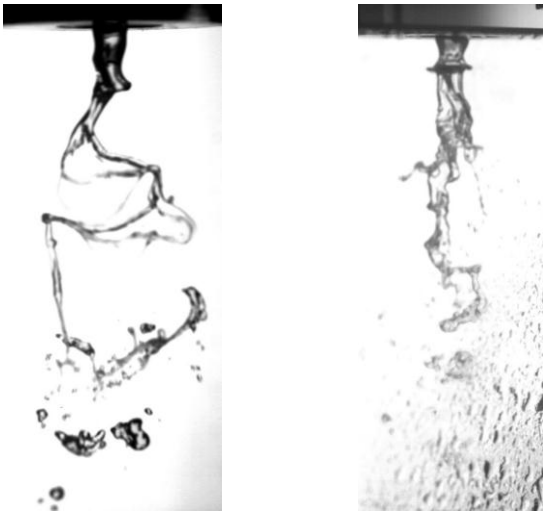

Figure 1: Instability of a liquid jet in airblast atomization for: a) Ug = 14 m/s, Ul = 0.25 m/s; b) Ug = 18.7 m/s, Ul = 0.31 m/s. a) KH wave is non-axisymmetric ; b) KH wave is axisymmetric.

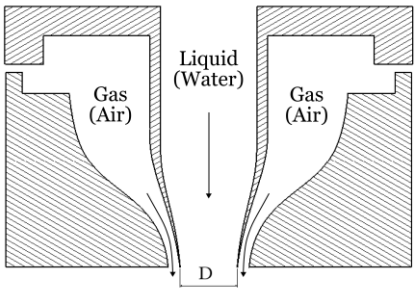

Figure 2: Sketch of the coaxial injector used in experimentations, not to scale. Diameter D is 8 mm; gas stream thickness Hg = 7.4 mm.

Air and water are injected through smooth convergent nozzles (figure 2), in order to reduce the intensity of perturbations.

Liquid velocity is varied from 0.18 m/s to 0.5 m/s and gas velocity is varied from 11.7 m/s to 18.7 m/s. These ranges of liquid and gas velocity correspond to the optimal conditions for visualization of the large scale phenomenon without a huge number of parasite stripping droplets. The structure of the intact flapping liquid jet is then clearly identifiable and image processing is made easier.

As seen in figure 1a, the liquid jet displays large oscillations; this phenomenon is identified as the large scale instability or flapping. This oscillation is three dimensional, and a single picture is not sufficient to describe unambiguously the spatial displacement of the jet.

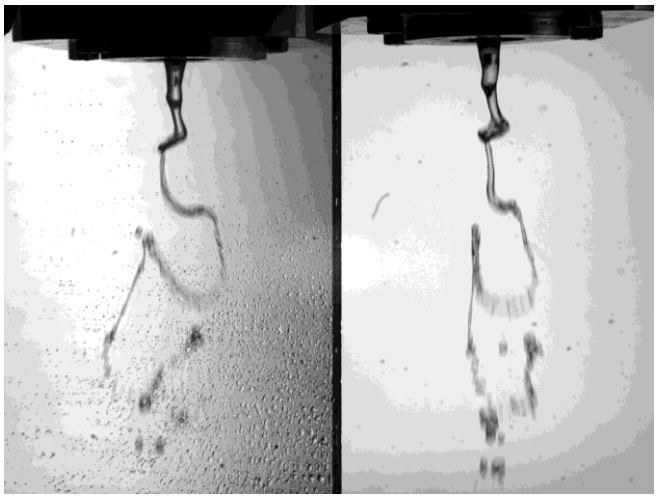

Figure 3: Visualization of the liquid jet via side and front view.

Figure 3 represents in the same picture the side (left) and front (right) view of the jet. This picture is obtained by means of a 45° angled mirror placed on the side of the jet, and a high-speed camera Vision Research Phantom V12 at a frequency of 1000 Hz. The frequency is the lowest for which we can time-resolve the phenomena. A sketch of this set-up is shown below in figure 4.

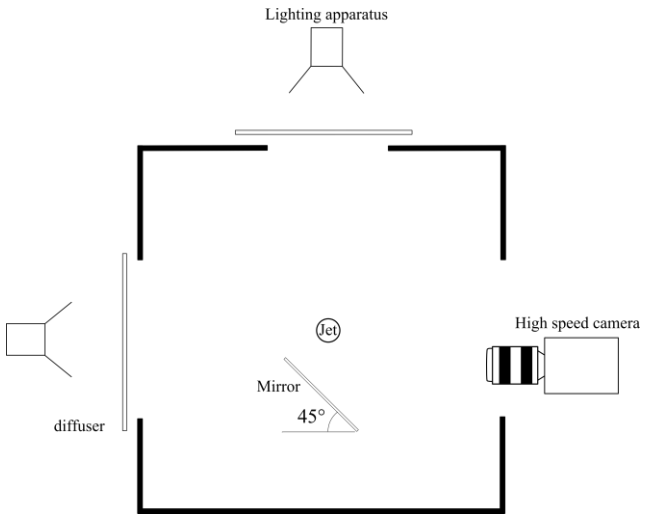

Figure 4: Sketch of the experimental set-up.

Data processing is then applied to these pictures. The interface for treatment used in this study is Matlab. For each picture and each view, droplets and liquid lumps not directly connected to the nozzle liquid tip are eliminated by use of a connexity algorithm. Two dimensional interface of the jet is then extracted, and calculation of the center of the jet for each projection of the jet is then carried out. Three dimensional coordinates of the center of the jet are then stored simultaneously with other data like interface profile. A kind of temporal database is then obtained by this method, which provides temporal geometric data: this data is used to obtain not only the flapping frequency, but also the spatial evolution of the amplitude of the jet, statistics on liquid jet break-up and radial displacement.

The initial K-H instability can give rise to unstable modes of the form $e^{i(kx-\omega t + n\theta)}$, where k is the wavenumber, ω is the frequency and *n* determines the angular symmetry of the mode. Axisymmetric modes correspond to n=0, while helical modes can correspond to either n=-1 or n=1. Determination of the nature of the unstable modes of this K-H instability can be carried out by computing the inter correlation product between the left and right profiles of the jet, on a single view (front or side view). This calculation has to be carried out over the region of effective presence of K-H waves. This region can be determined with the following criterion: the radial displacement of the center of the liquid jet has to remain smaller than the liquid jet radius R. The flapping instability starts at the downstream distance where this radial displacement becomes larger than R.

Mean interface signals are computed and subtracted to each instantaneous interface signal, in order to examine the K-H instability waves around the mean jet thinning due to gravity acceleration. A correlation coefficient is then calculated between both profiles with this expression (corr2 function under Matlab):

$$C = \frac{\sum_m \sum_n (A_m - \bar{A})(B_m - \bar{B})}{\sqrt{\left(\sum_m \sum_n (A_m - \bar{A})^2\right)\left(\sum_m \sum_n (B_m - \bar{B})^2\right)}}$$

where A and B represent interface signals, and (m,n) dimensions of these signals; r will be a scalar between -1 and 1: C=-1 if signals are of opposite phases, and C=1 if signals have the same phase. This criterion gives an indication if waves are symmetrical (-1) or not (1). A statistical distribution obtained with independent temporal pictures is computed. Distributions are computed for various control parameters (liquid and gas velocity).

Another interesting characteristic of the large scale instability is the spatial evolution of the amplitude. With our database, radial distance of the jet to the injection axis can be computed. A statistical analysis at each vertical downstream position gives a statistical radial position of the center of the jet. The spatial variation of the amplitude is then computed from this statistical data. At each vertical position downstream the injector, a cumulative sum is computed and the position for which x percent of the number of events is reached is retained as the width, or amplitude, of the jet. This processing is a way to characterize the statistical behavior of the jet, by eliminating rare events.

Results and Discussion

Kelvin-Helmholtz mode investigation

The symmetry of the unstable K-H mode can be discussed with the data of figure 5. This figure represents the normalized distributions of correlation coefficient r as a function of gas velocity U_g. Grey levels represent the normalized proportion of each value of correlation coefficient. A clear transition is visible in this figure: for gas velocities below 14 m/s, correlation coefficient is close to 1, while above 14 m/s, r is close to -1. Around a gas velocity of 14 m/s, distributions are saddle-looking, with coexistence of two kinds of signals, phased and non-phased.

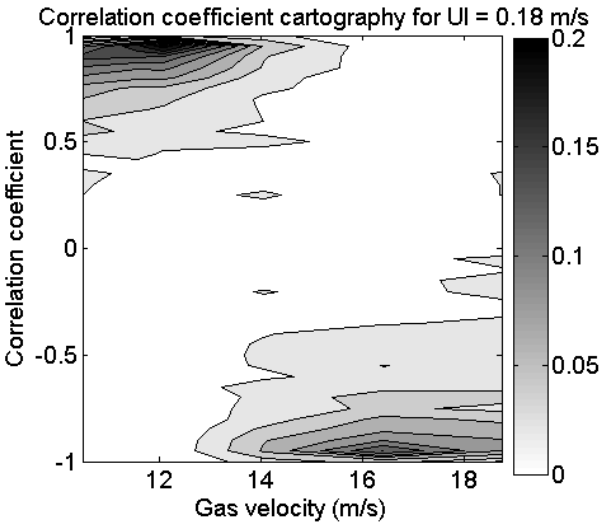

Figure 5: K-H wave mode dependency on gas velocity for a liquid velocity equal to 0.18 m/s.

Signals in phase opposition indicate that a symmetrical mode is detected. On the contrary, a single helical mode, n=-1 or n=1, would generate two signals in phase, independent of the projection plane. A superposition of two modes n=1 and n=-1 having the same amplitude would generate a mode with a plane of symmetry, i.e. a mode having the same symmetry as the flapping instability: for this mode the interface signals can be in phase or not, depending on the orientation of the plane of symmetry relative to the camera. This orientation has been observed to change randomly over the course of measurements. As a consequence, if such a mode is present, the distribution should be saddle-looking, meaning that it has maxima for both n=1 and n=-1. This is the case on figure 5 for Ug between 13 and 15 m/s. At gas velocities between 11 and 13 m/s, this kind of distribution is not observed, and the instability should therefore be dominated by helical modes alone. Conversely, for U_g>16 m/s, the anti-correlation of both sides suggests the dominance of a symmetric n=0 mode. Saddle distributions are only an evidence of the coexistence of different modes. This is probably due to the growth rates of axisymmetric and helical modes being very close at this transitional gas velocity (see Matas et al 2013). The same tendency is observed for other liquid velocities (see figures 6, 7 and 8).

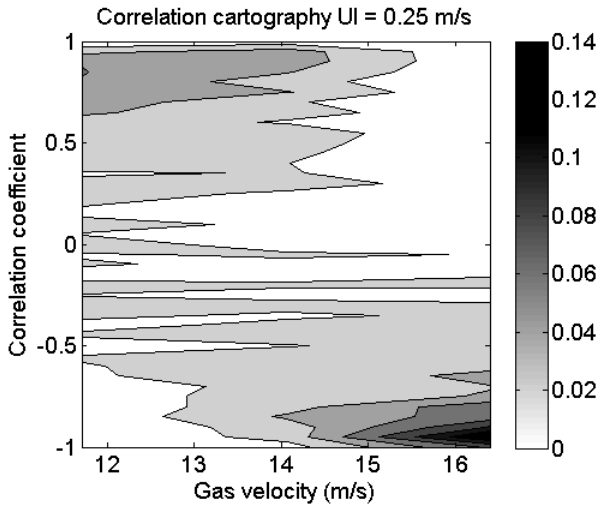

Figure 6: Correlation of wave profiles as a function of air velocity, for a liquid velocity U_l = 0.25 m/s.

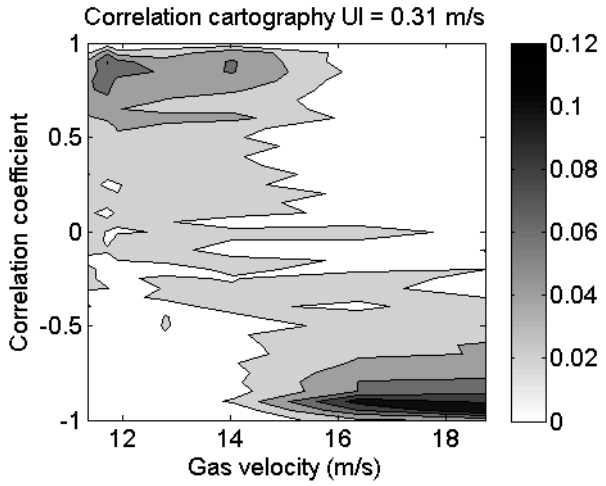

Figure 7: Correlation of wave profiles as a function of air velocity, for a liquid velocity U_l = 0.31 m/s.

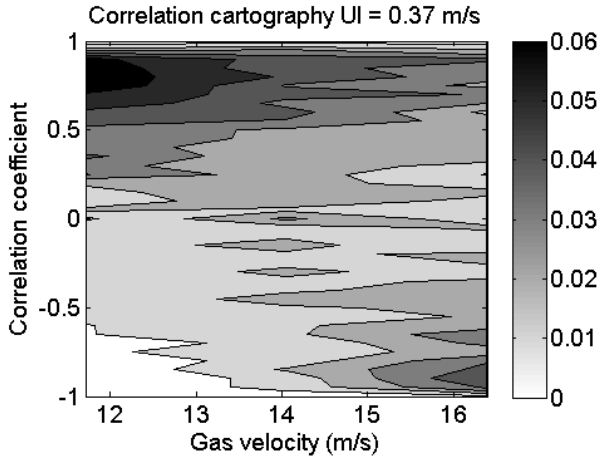

Figure 8: Correlation of wave profiles as a function of air velocity, for a liquid velocity U_l = 0.37 m/s.

Amplitude of large scale instability

We now look at the variation of the amplitude of the liquid jet. Figures 9 and 10 represent the measured radial displacement of the liquid jet centre as a function of the vertical distance. These figures show the spatial growth of the radial amplitude of the jet with vertical distance from injector and for different liquid velocities. Measurements stop at the break-up length of the jet. For each gas and liquid velocity a linear behaviour is seen far from the injector. For low downstream distances, it can be seen that an increase in gas velocity induces an increase in the amplitude of the large scale instability. For larger distances the maximum amplitude is roughly obtained for intermediate gas velocities. Note however that since the break-up length depends on gas velocity, all curves do not extend until the same downstream distance, and comparison of amplitude at large z is more difficult.

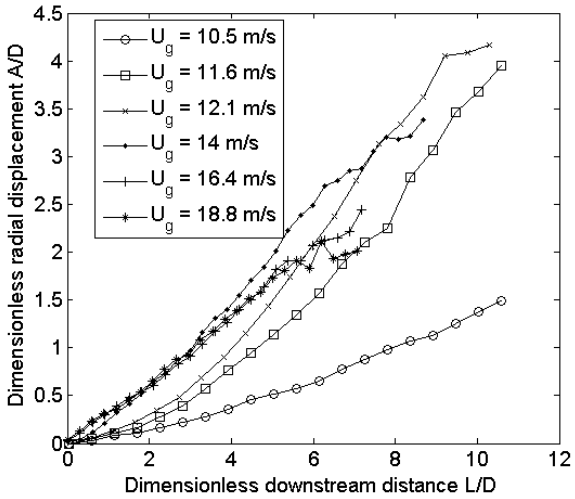

Figure 9: Dimensionless amplitude of the liquid jet as a function of dimensionless downstream distance to the injector for various U_g and U_l = 0.18 m/s.

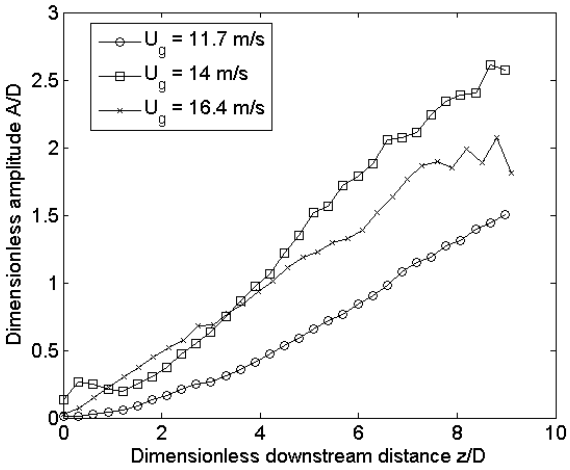

Figure 10: Dimensionless amplitude of the liquid jet as a function of dimensionless downstream distance to the injector for various U_g and U_l = 0.37 m/s.

The spatial variation of the amplitude shows how much the liquid jet is radially displaced, and more precisely how

the large scale instability is amplified. As said previously in the experimental methodology, this data is obtained with only the liquid jet bulk, no droplets are present nor effect the measure. It ensures that a possible aliasing of stripping droplets is avoided.

We believe that the flapping instability is triggered by a non-axisymmetric perturbation upstream (typically a non–axisymmetric KH wave), which induces non-axisymmetric gas flow recirculations on either side of the jet (see figure 11). The gas jet is then deflected in a non symmetric way on either side.

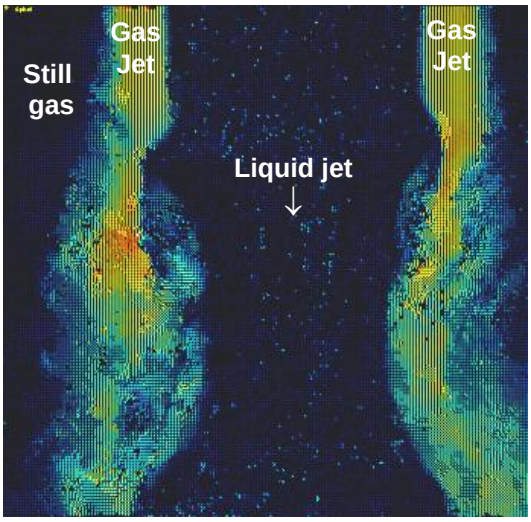

Figure 11: PIV visualization of gas flow around the liquid flow: non axi-symmetric KH wave induce non-axisymmetric recirculations.

We now try to capture the variation of the amplitude induced by this mechanism. We note A the amplitude and T the typical time over which the destabilization takes place. We write that for a segment of liquid jet of length λ the horitzontal acceleration A/T^2 is caused by the drag of the deflected gas jet:

$$\lambda.R^2.\rho_l.\frac{A}{T^2} \approx \rho_g.U_g^2.H_g.R$$

We consider here that the drag $\rho_g U_g^2$ is exerted on a surface $H_g R$, i.e. we consider that the whole gas jet is deflected and hits the liquid jet over a width R and a downstream extent H_g. The typical time T is basically the free-fall time:

$$T = \frac{U_l}{g}\left[\sqrt{1+\frac{2.z.g}{U_l^2}} - 1\right]$$

where U_l is the initial velocity of the liquid jet, g gravity and z the vertical distance to the liquid injector nozzle.

This yields the following amplitude:

$$A = M.\frac{H_g}{\lambda.R}.\frac{U_l^4}{g^2}.\left[\sqrt{1+\frac{2.z.g}{U_l^2}} - 1\right]^2 \qquad (1)$$

where M is the dynamic pressure ratio $M = \rho_g U_g^2/\rho_l U_l^2$.

This expression is a function of the wavelength λ, which is not known. Experimental evidence indicates that λ increases with vertical distance to the injector nozzle. In a first approach, we measure λ and inject the value experimentally measured in the expression for A. We have assumed that vertical acceleration is controlled by gravity: this may not be true for large gas velocities, when the gas jet may also induce a vertical acceleration of the liquid structure. In figure 12 we show measurements of the vertical acceleration of the liquid structure, as a function of gas velocity. For a given set of conditions, the acceleration is roughly independent of z. Figure 12 also shows that it does not depend on liquid velocity, but increases strongly with gas velocity. Finally, note that for Ug>12 m/s, this acceleration is much larger than *g*.

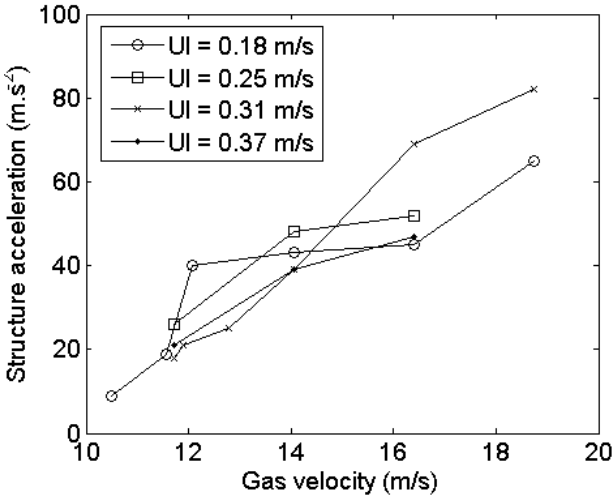

Figure 12: Acceleration of the liquid structure with gas and liquid velocity.

In figure 13, both measurement and prediction of the radial displacement of the liquid jet are shown as a function of vertical distance to the injector for Ug = 11.7 m/s and Ul = 0.37 m/s. The dotted curve corresponds to the prediction with a liquid jet accelerated by gravity: this prediction overestimates the amplitude. The dash-dotted curve assumes that the liquid structure travels at a constant Ul: this curve underestimates the experimental amplitude. Finally, the dashed curve takes into account the experimentally measured acceleration of figure 12: this estimates is roughly consistent with the experimental value. It captures the good order of magnitude of the amplitude, even though the exact shape of the curve A(z) is not captured. Figure 14 shows the same comparison for different gas/liquid velocities, namely Ug = 18.7 m/s and Ul = 0.18 m/s: again, the prediction with the experimental acceleration is the one closest to the experimental data.

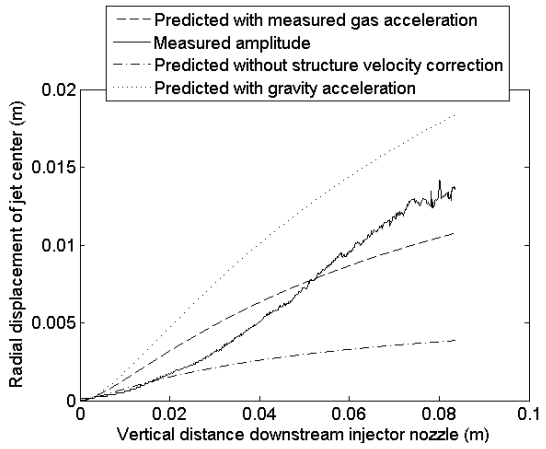

Figure 13: Predicted and measured radial displacement for U_g = 11.7 m/s and U_l = 0.37 m/s. Predictions with different hypotheses.

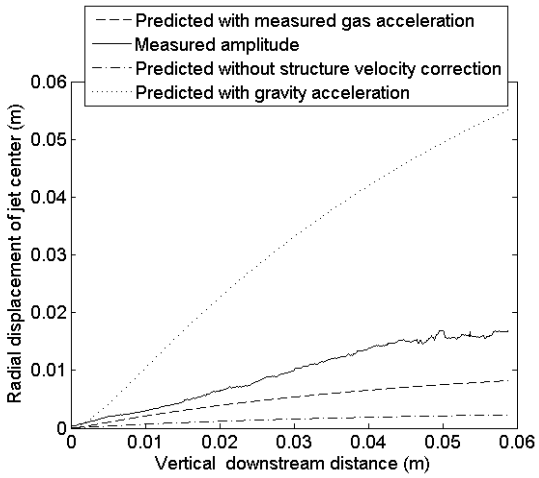

Figure 14: Predicted and measured radial displacement for U_g = 18.7 m/s and U_l = 0.18 m/s. Predictions with different hypotheses.

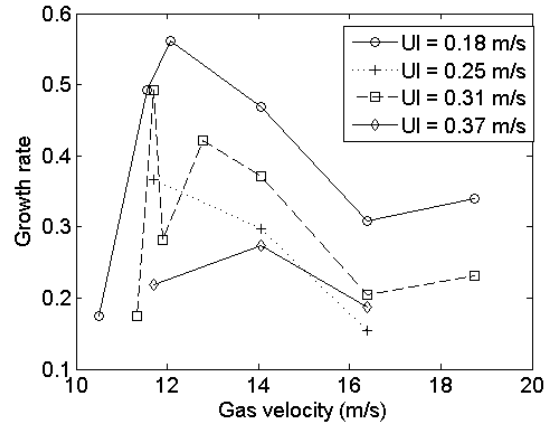

Figure 15: Amplitude gradient of the liquid jet dA/dz as a function of gas velocity.

Finally, figure 15 shows the amplitude gradient of the liquid jet dA/dz as a function of gas velocity, for several liquid velocities. This quantity represents the slope of the cone described by the liquid jet. More precisely it is computed between the distance where the jet centre departs from the axis, and the distance of jet break-up.

Except for the lowest gas velocities, dA/dz consistently decreases as a function of gas velocity. We believe this decrease can be related to the pattern of figures 5 to 8, where a switch from a non axi-symmetric (i.e. favourable) to a symmetric mode (i.e. non favourable) is seen.

Conclusions

A study on the symmetry of K-H modes has been made in a coaxial jet configuration. As gas velocity is increased, a switch from a non-axisymmetric to a symmetric pattern is observed. Non axi-symmetric modes are suspected to be responsible for the triggering of the flapping instability. Measurement of the amplitude of the flapping instability has been carried out for a range of liquid and gas velocities. A simple model captures the magnitude of this amplitude. The variation of the amplitude as a function of gas velocity is interpreted in terms of a switch from upstream non-axisymmetric KH modes to axisymmetric KH modes.

Acknowledgements

The research leading to these results has received funding from the European Union Seventh Framework Programme (FP7/2007-2013) under grant agreement n°265848 and was conducted within the FIRST project.

References

J. Eggers and E. Villermaux, “Physics of liquid jets", Rep.Prog.Phys., 71 036601 (2008).

M. Hong, A. Cartellier and E. J. Hopfinger, “Atomization and mixing in coaxial injection”, Proc. 4th Int. Conf. on launcher technology, Liège, Belgique (2002).

J. Lasheras and E.J. Hopfinger, “Liquid jet instability and Atomization in a coaxial gas stream”, Annu. Rev. Fluid Mech., 32 275-308 (2000).

P. Marmottant and E. Villermaux, “On spray formation”, J. Fluid Mech., 498, 73 (2004).

Marty S., Matas J.-Ph., Cartellier A., Study of a liquid-gas mixing layer: Shear instability and size of produced drops, Comptes Rendus Mécanique, 341, Issue 1-2, 26-34 (2013).

Matas J.-Ph., Cartellier A., Flapping instability of a liquid jet, Comptes Rendus Mécanique, 341, Issue 1-2, 35-43 (2013).

J-P Matas, S. Marty and A. Cartellier, “Experimental and analytical study of the shear instability of a gas-liquid mixing layer”, Phys. Fluids, 23 094112 (2011).

L. Rayleigh, “On the stability, or instability, of certain fluid motions,” Proc. London Math. Soc. 11, 57 (1879).

Varga, C.M., Lasheras, J.C. and Hopfinger, E.J., Initial break-up of a small-diameter liquid jet by a high-speed gas stream, J. Fluid Mech., 497, (2003).